



# Macroaggregates of loam in sandy soil show little influence on maize growth, due to local adaptations of root architecture to soil heterogeneity

Eva Lippold · Maik Lucas · Toni Fahrenkamp ·  
Steffen Schlüter · Doris Vetterlein

Received: 22 October 2021 / Accepted: 28 March 2022  
© The Author(s) 2022

## Abstract

**Aims** Root hairs and lateral growth are root traits among many which enable plants to adapt to environmental conditions. How different traits are coordinated under local heterogeneity, especially when two or more environmental factors vary in space, is currently poorly understood. We investigated the effect of heterogeneity on root system architecture of maize in response to the presence of loamy macroaggregates, which come along with both, increased penetration resistance and nutrient availability, i.e., two important environmental factors shaping root system architecture. The comparison between a mutant with defective root hairs and the corresponding wild type made it possible to investigate the importance of root hairs in the adaptation strategies of plant roots to these factors.

**Methods** Changes in root growth and root distribution with respect to macroaggregates were investigated using X-ray computed tomography. The wild-type of *Zea mays* L. was compared with the root hair defective mutant (*rth3*) to investigate the importance of root hairs in addition to adaption of root architecture.

**Results** The presence of aggregates lead to increased root length and branch densities around aggregates, while only a few roots were able to grow into them. Thereby, wildtype and *rth3* were influenced in the same way. Aboveground biomass, however, was not affected by the presence of macroaggregates, as compared to controls with homogeneously distributed loam.

**Conclusions** Macroaggregation of loam in sandy soil shows little influence on maize growth, due to local adaptations of root architecture to the heterogeneity in nutrient availability and penetration resistance caused by the aggregates.

---

Eva Lippold and Maik Lucas shared first authorship

---

Responsible Editor: Andrea Schnepf.

---

**Supplementary Information** The online version contains supplementary material available at <https://doi.org/10.1007/s11104-022-05413-5>.

---

E. Lippold (✉) · M. Lucas · T. Fahrenkamp · S. Schlüter ·  
D. Vetterlein  
Department of Soil System Science, Helmholtz Centre  
for Environmental Research – UFZ, Halle (Saale),  
Germany  
e-mail: [eva.lippold@ufz.de](mailto:eva.lippold@ufz.de)

**Keywords** X-ray CT · Imaging · Soil structure ·  
Root system architecture · Root plasticity · Root hairs

## Abbreviations

CT    computed tomography  
*rth3*    root hair defective mutant  
S    sand  
WT    wild-type

## Introduction

Soils are heterogeneous and complex mixtures of organic matter, mineral particles, and pore space. Their functionality is determined by the spatial arrangement of these components on different scales, i.e. by the soil structure (Ritz et al. 2004; Portell et al. 2018; Rabot et al. 2018; Kravchenko and Guber 2021). Roots interact with the soil and its structure. This interaction is governed by several environmental factors, which influence the development of roots and shape the root system architecture, making roots highly adaptive to the local environment (Downie et al. 2015; Morris et al. 2017). Well known examples of these factors are water stress and mechanical impedance (Bengough et al. 2011; Correa et al. 2019; Colombi et al. 2018).

Root elongation decreases drastically in response to increasing penetration resistance and decreasing matric potential (Bengough et al. 2011; Veen and Boone 1990; Dexter 1986). Hence, root penetration into aggregates, with their increased resistance to penetration (Becher 1992), is likely to be impaired compared to their growth into the surrounding soil matrix. It was shown, that increasing aggregate size, density, and strength lead to reduced root growth and thus reduced aggregate size may be beneficial for root growth (Logsdon 2013; Freitas et al. 1999).

However, not just physical properties can change the growth of roots and resulting root system architecture. To assimilate nutrients efficiently, plants have developed a range of adaptive responses (Hodge 2004), e.g. plant roots may respond to localised phosphorus sources with locally increased root elongation and increased branch density (Flavel et al. 2014; Gao et al. 2019a; Robinson 1994b).

In addition, root hairs are assumed to be an important feature for roots to respond to soil heterogeneity in terms of penetration resistance and nutrient availability. For example, root hairs can be used to anchor during root establishment and thus overcome soil penetration resistance (Bengough et al. 2016; Haling et al. 2013), while they also increase the availability of nutrients like phosphorus (Bengough et al. 2011; Vetterlein et al. 2021).

X-ray  $\mu$ CT has proven to be a useful tool to analyse such root morphological responses to local changes in soil structure as well as to the amount and distribution of nutrients (Flavel et al. 2014; Gao et al. 2019a;

Lucas et al. 2019; Colombi et al. 2017; Burr-Hersey et al. 2017; Blaser et al. 2020).

In this study, we analyzed the combined effect of heterogeneity in soil penetration resistance and nutrient availability on root system architecture. This is achieved by examining plant growth in columns with two sandy substrates with X-ray  $\mu$ CT. Though the average soil texture is identical, one of these substrates contains large sized loamy aggregates, while the other corresponds to a standardized, homogenized laboratory soil, in which the loam is sieved and evenly distributed. These loamy aggregates induce areas of larger penetration resistance due to their stability and thus may reduce root elongation. On the other hand, due to the higher cation exchange capacity and the higher content of Fe-(hydr)oxides in these loamy aggregates, there are higher concentrations of potentially available P. Plant roots therefore may prefer to grow towards larger loamy aggregates, which contain higher concentrations of P (Gao et al. 2019a; Robinson 1994a).

In addition, we investigated the importance of root hairs for the adaption in root system architecture. This is addressed by using two genotypes of *Zea mays* L. The first is the wild-type (WT) and the second is a corresponding mutant defective in root hair elongation (*rth3*) (Hochholdinger et al. 2008).

We hypothesized that 1) maize roots grow towards loamy aggregates to maintain sufficient nutrient uptake for plant growth, but 2) show reduced root growth into them because of higher penetration resistance. Thus, 3) total plant growth in aggregated substrates will be reduced, which is 4) especially true for hairless mutants, as they may not be able to overcome the penetration resistance of the aggregates.

## Materials and methods

### Experimental design

The experiment was set up as a two factorial, randomized design with three replicates. The term replicates refers to individual soil columns. Factor one was substrate with two levels i.e. aggregated and sieved. Factor two was *Zea mays* L. genotype with two levels namely B73 wild-type (WT), and the corresponding root hair defective mutant (*rth3*).

## Substrates varying in aggregation

Both substrates are a mixture of 83.3% quartz sand and 16.7% loam taken from a Haplic Phaeozem. The major difference between the two substrates is the soil structure. As described in Vetterlein et al. (2021), the aggregated substrate was created by mixing quartz sand and unsieved loam for a field experiment using a heavy double deck vibrating screen and used as such. For technical reasons, stable large sized loam aggregates (approx. 10 vol%) are created in the otherwise homogenous sandy substrate. The sieved substrate for laboratory experiments was generated by sieving the aggregated loam down to 1 mm using a cylindrical handhold sieve before mixing with the quartz sand. This was done to achieve an as homogenous mixture in column experiments as possible. The two substrates will be referred to as Aggregated and Sieved. The penetration resistance in the sieved substrate was measured in parallel experiments under identical conditions and amounted to 0.08 MPa (Roskopf et al. 2021). The penetration resistance of individual macroaggregates embedded in the aggregated substrate was not measured. Unsorted, unmixed loam packed at a bulk density of  $1.27 \text{ g cm}^{-3}$  had a penetration resistance of 0.15 MPa in the moisture range of the experiment (Roskopf et al. 2021). The macroaggregates are supposed to have a much higher penetration resistance due to higher bulk density and particularly high stability as they endured the vigorous mechanical agitation of the vibration screen.

Both substrates were fertilized with fertilizer solutions according to Vetterlein et al. (2021). A description of the initial soil chemical composition can be found in the same publication. To achieve a homogeneous distribution of nutrients the material was sieved again after drying with a handheld sieve after fertilization. As the loam aggregates in the aggregated treatment would have been partly destroyed in this manner, they were removed with a sieve from the mixture prior to fertilization and then added again after sieving. Following the packing protocol described in Lippold et al. (2021b), acrylic glass cylinders with an inner diameter of 7 cm and a total height of 25 cm were filled up to 23 cm height with the investigated substrates to a bulk density of  $1.47 \text{ g cm}^{-3}$ . Surface sterilized maize seeds were placed at 1 cm depth. Surface was covered with quartz gravel to reduce evaporation. The columns

were irrigated from top and bottom in the night before day 2, 5, 9, 13, 15, 17, 19, and 21 after sowing to an average volumetric water content of 18%. Watering intervals were shortened with increasing plant size to avoid drought stress. All plants were grown in a climate chamber for 21 days with 12 h light per day and a light intensity of  $350 \mu\text{M/m}^2\text{s}$  of photosynthetic active radiation. Temperature was set to 22 °C during the day and 18 °C at night with constant relative humidity of 65%.

## Shoot biomass sampling and nutrient analysis

On day 22, shoots were cut off and dried at 65 °C for 72 h. After determination of shoot dry weight the material was ground down to fine powder. C/N was analysed by combustion with a CN elemental analyzer (vario EL cube, Elementar, Germany). Phosphorus (P), Potassium (K) and Calcium (Ca) were determined by ICP-OES (ARCOS, Spectro AME-TEC, Germany) after pressure digestion with  $\text{HNO}_3$  in a microwave (Mars 6, CEM Corporation, USA). To compare the uptake of a highly mobile nutrient with one of low mobility without the confounding impact of plant growth, the Ca:P ratio in the shoot biomass was assessed for each replicate (Lippold et al. 2021b).

## Destructive sampling of roots and substrate

After cutting the shoots, the soil was pushed out of the acrylic column. The soil was sliced into layers to separate areas scanned with X-ray CT from unscanned areas (0–23 cm depth). The layers were placed on a 0.63 mm sieve and roots were washed out carefully with deionised water after taking 30 g of each layer for substrate analysis. Roots were stored in 50% ethanol solution (Rotisol). Subsequent, roots were scanned on a flatbed scanner at 720 dpi (EPSON perfection V700). Thereafter, root traits were analysed using the software WinRhizo 2019 (Regent Instruments, Canada). The material from each layer for substrate analysis was pooled again to have one sample per biological replicate. However, former aggregates and fine material was bulked separately. Samples were air dried for 72 h and sieved to 1 mm. Plant available P was determined by the CAL-method (von Schüller 1969).

## Leaf area

Effects of the different treatments on plant growth over time were investigated by measuring leaf area each time watering was done. Width and length of every leaf was recorded. All leaves were scanned on a flatbed scanner at day of harvest and then measured in colour classification mode in WinRhizo. To estimate the leaf area during the experiment and correct for the typical shape of a leaf, these results were then used to create a linear model using R. The best model fit was achieved with the following Model (adjusted  $R^2 = 0.991$ ):

$$Area_{leaf} = 0.723 * Width_{leaf} * Length_{leaf}$$

## X-ray $\mu$ CT

X-ray tomography was performed with an industrial  $\mu$ CT (X-TEK XTH 225, Nikon Metrology) at 160 kV and 296  $\mu$ A. A total of 2748 projections with an exposure time of 500 ms each were acquired during a full rotation of the columns. Samples were placed 18.2 cm away from the X-ray source during image acquisition. A 0.5 mm thick copper filter was used between the source and the column in order to reduce beam artefacts. A lead shield with a window (2.5\*2.5 cm) was placed to minimize diverging photons outside the field of view, i.e. to the plant shoot and in the soil outside the field of view. With this setup, the dose per scan measured with a RPL dosimeter in the center of the column amounts to 1.2 Gy (Lippold et al. 2021a). X-ray CT scanning was performed at day 21 after planting (DAP) during night time so as to not interfere with plant photosynthesis. Columns were scanned at two depths interval making sure that an overlapping region was present. Each depth interval scan took 23 min to complete. The obtained images were reconstructed into a 3D tomogram having a voxel size of 45  $\mu$ m and an 8-bit greyscale via a filtered back projection algorithm with the CT Pro 3D software (Nikon metrology). During the 8-bit conversion, the greyscale range was normalized with a percentile method which sets the darkest and brightest 0.2% voxels to 0 and 255, respectively.

## Segmentation of roots

The images were processed and roots were segmented with the Routine workflow of Gao et al. (2019b). The basis of this workflow is the use of the ‘Tubeness’ plugin (<https://imagej.net/Tubeness>) in Fiji (Schindelin et al. 2012; Rueden et al. 2017). This allows the use of the most common feature of all sized roots, which is their cylindrical shape. Prior to the feature extraction, image processing steps are performed, which 1) normalise the grey values with the ‘Attenuation correction’ plugin in Fiji and 2) reduce the noise by using a fast, unbiased 3D Non-Local Means filter (Tristán-Vega et al. 2012) in ITK.

## Segmentation of aggregates

A new protocol was developed to segment loamy aggregates in the sandy substrate. This starts using the normalized and filtered image from the Routine script. This offers already a good contrast between aggregates and sand particles (Fig. 1). Afterwards a “White Top Hat” filter of the plugin MorphoLibJ (V1.4.1) in Fiji (Legland et al. 2016) is used. The result is subtracted from the filtered image and a threshold is applied to this difference image using Otsu’s method (Otsu 1979). As some of the aggregates contained some macropores, 3D closing with a radius with a cube of 5x5x5 is used to close these holes. A 3D watershed transform of the binary image is used finally to split touching aggregates. These two functions are also implemented in the MorphoLibJ plugin.

## Analysis of local changes in root growth

The “Skeletonize” and “Local Thickness” functions were used to compute the root length, root branching points (junctions) and root diameters from the resulting root image of Routine. To describe the local changes in root growth in response to aggregates in a holistic way (Fig. 1), we analyzed 1) root length as well as root branch density, root diameter and root volume as a function of aggregate distance, 2) the distribution of aggregates and roots with respect to the column wall and 3) root length density within aggregates and in the surrounding sand substrate. To achieve 1) and 2) the Euclidean distances maps of the aggregates and the column wall was computed and

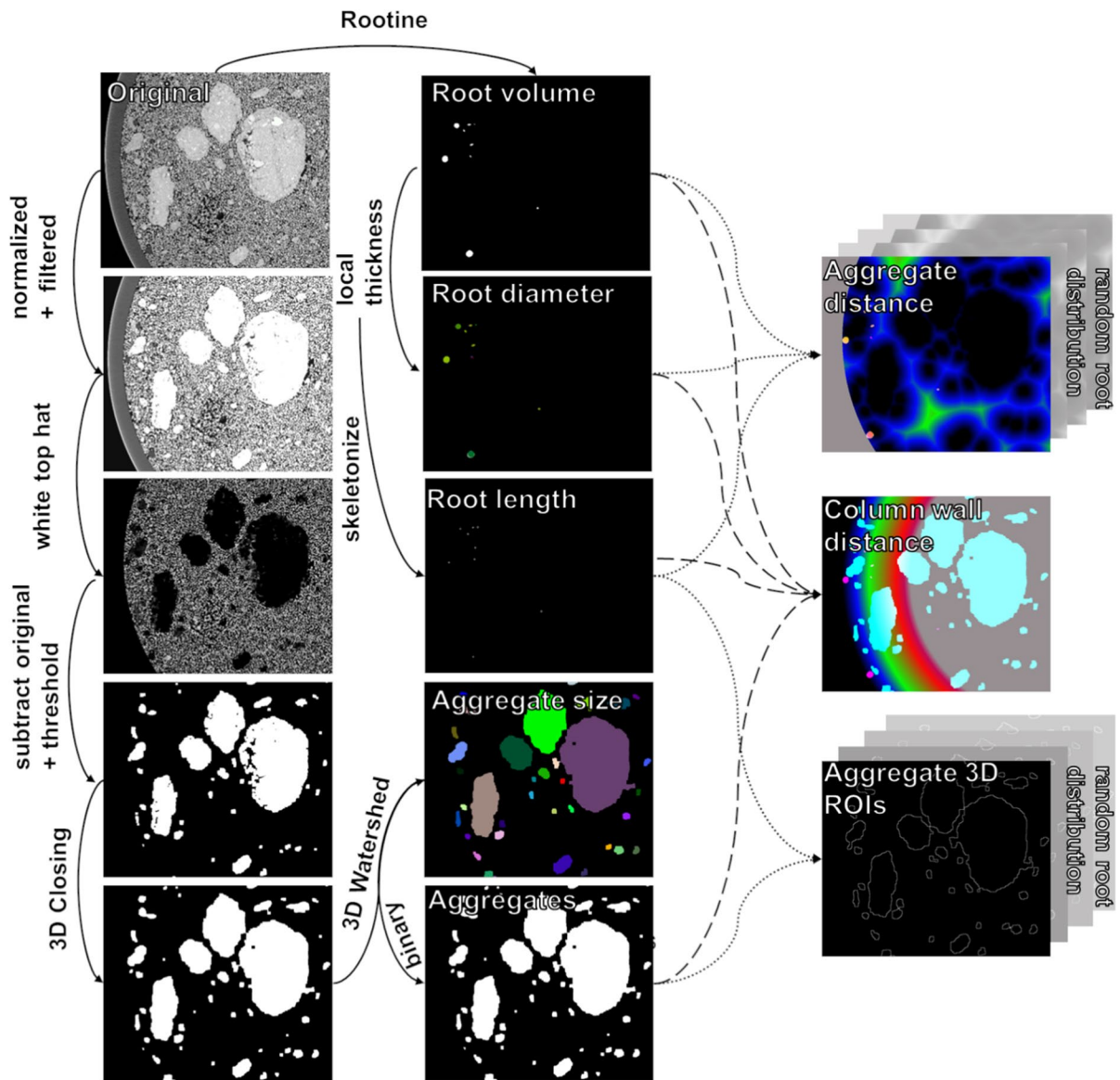


**Fig. 1** Workflow for the segmentation of aggregates and analysis of root distribution in relation to aggregates. Aggregate distance refers to the distance from any soil voxel outside an

aggregate to the nearest aggregate, likewise column wall distance refers to the distance from any soil voxel to the nearest voxel of the column wall

combined with the root images as described in Lucas et al. (2019). The 3D ROI Manger was used to compute 3) (Ollion et al. 2013).

#### Random root distribution

A response of root growth to certain soil features can be gauged in several ways. A common approach is compare measured root traits against a benchmark

with identical average properties in which either the location of roots (Phalempin et al. 2022) or the location of soil features (Colombi et al. 2017) are randomized. Here we adopt and modify the approach of Colombi et al. (2017). To compare the resulting root distributions with a root system not influenced by aggregates we generated random, but realistic root distributions from root images of the same data set. For this, the root images of the sieved treatments were



used, by rotating the images stepwise three times by 90°. Thus, twelve root systems per column were generated for which the relative positions of roots and aggregates were randomized and corresponding root distributions were calculated.

The whole workflow of aggregate segmentation and image analysis can be found as ImageJ macro file in the Supplementary Material.

## Statistics

Standard errors and mean values of the three replicates for each combination of maize genotype (WT and *rth3*) and soil substrate (Sieved and Aggregated) are provided. The influence of the two factors on leaf area and root length density at different locations (matrix, aggregates of different sizes) at the end of the experiment were additionally evaluated by two-factorial ANOVA's in conjunction with Tukey's HSD test. The assumptions of the different models were

visually assessed by evaluating plots of residuals (residuals vs residuals, QQ plot of standardized residuals). For all statistical analyses the software R 4.02 and the package agricolae (de Mendiburu 2017) were used.

## Results

### Influence on total plant and root growth

The first set of analysis aimed to reveal changes in total plant and root growth affected by plant genotype and aggregation. On average WT plants developed larger leaf area than *rth3* plants in both substrates beginning from day 10 after planting until the day of harvest (Fig. 2b). However, significant differences between the sieved soil and the aggregated field soil could not be detected for neither of the genotypes (Fig. 2b,  $p = 0.28$ ), although leaf growth after day 17 seem to be higher for plants growing in the aggregated

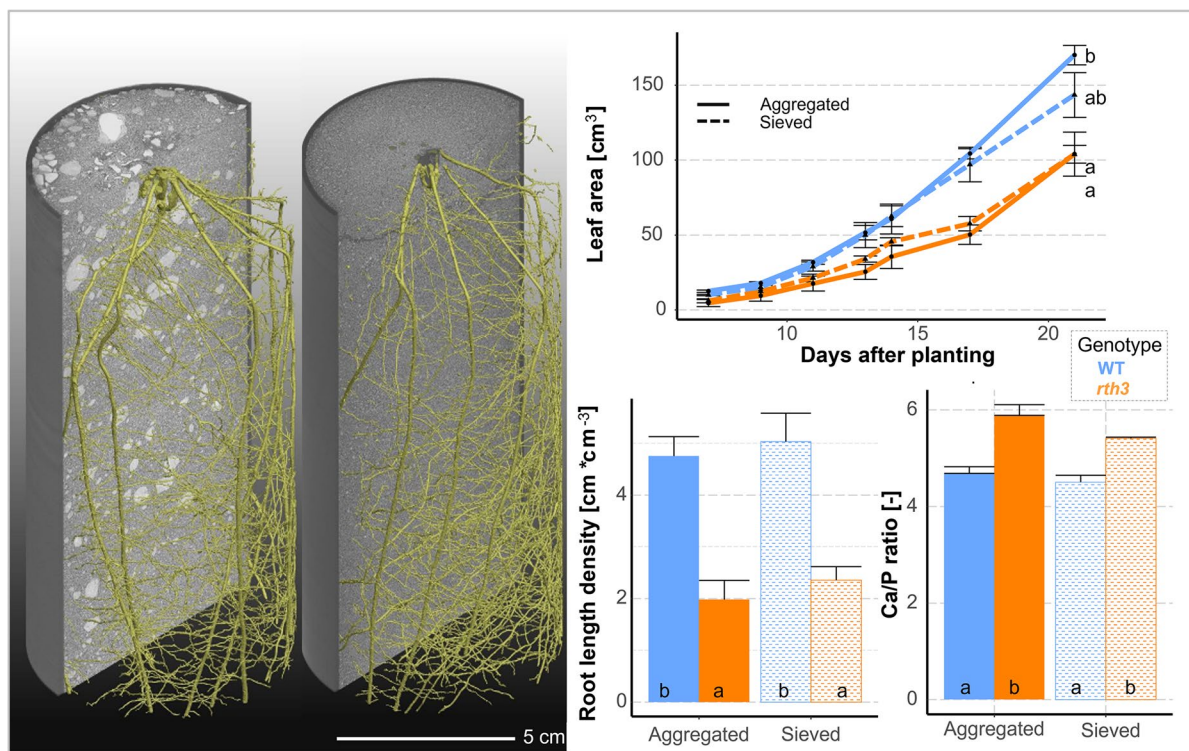


**Fig. 2** Rendered 3D images of root system in aggregated and sieved substrate (A). Plant growth (leaf area) over time (B). In addition, root length density (C) and Ca/P-ratio (D) at the end of the experiment. Different letters indicate significant differ-

ences ( $p$  value  $< 0.05$ ). Compared are the genotypes of maize (WT = wildtype, *rth3* = root hairless variety) in the two substrates at the end of the experiment. Error bars show standard errors of the mean

substrate. The same is true for the observed root length densities (Fig. 2c), which were more than twice as high for WT compared to *rth3* but independent of substrate ( $p=0.41$ ). In addition, significant differences between substrates ( $p=8.19 \times 10^{-6}$ ) and between genotypes ( $p < 2 \times 10^{-16}$ ) were found for root diameters with *rth3* having thicker roots than WT and both genotypes having thicker roots in aggregated substrate (Fig. S1). The ratio between Calcium and Phosphorus in the shoot material was calculated as this is expected to be independent from any dilution by growth in contrast to individual tissue concentrations. The Ca:P ratio showed higher values for *rth3* as compared to WT ( $p=5.46 \times 10^{-5}$ ). The substrate, however, had only a tendency to significant differences ( $p=0.054$ ), which can be mainly related to difference in *rth3*, showing a tendency to higher Ca:P ratios in the aggregated substrate (Fig. 2D).

#### Local adaption of root traits in aggregated soil

The root length densities derived from X-ray CT data were in a good agreement with the WinRhizo data ( $R^2=0.99$ ), although approx. 14% of the maize roots could not be recovered by the 3D imaging technique (Fig. S2). Especially roots of the WT showed lower recovery rate within the CT images compared to the results from destructive sampling. This can be attributed to differences in root diameters between the two genotypes. In both substrates the average root diameter was significantly lower for the WT ( $p < 1 \times 10^{-5}$ ) and hence its recovery in X-ray CT images was more challenging. Especially in the diameter class  $<0.1$  mm root diameter was close to the resolution (2 voxels). In this diameter class root length of the WT was approx. Doubled compared to *rth3*, when measured destructively.

There was a significant decrease of root length density within aggregates (Fig. 3,  $p=0.015$  for *rth3* and  $p=0.002$  for WT). While the root length density in aggregates increased monotonously with increasing aggregate size for the WT, this was not true for *rth3*. Consequently, significantly lower root length densities could be found in aggregates  $>1$  mm<sup>3</sup> in columns of *rth3* compared to columns of the WT ( $p=0.01$ ).

From that data alone, it is not clear whether these differences were a response of adaptive root growth or simply arose from different volume fractions of

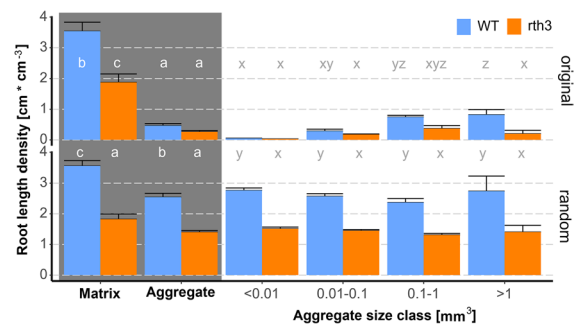


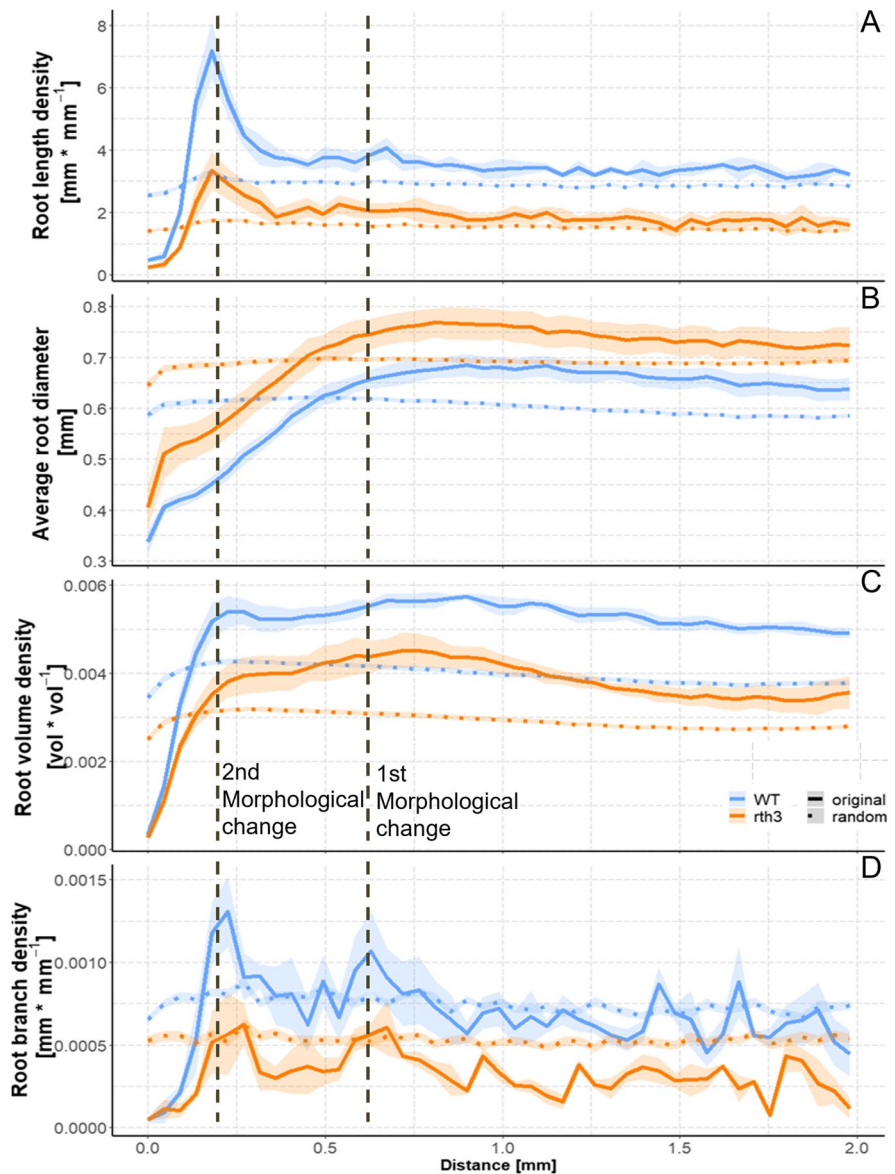
**Fig. 3** Roots in different locations. Different letters indicate significant differences ( $p$  value  $<0.05$ ). Differences in root length density between genotypes (WT = wildtype, *rth3* = root hair defective genotype) and spatial domains. Matrix vs aggregate and aggregates of different sizes were tested separately, which is indicated by different letters used (a, b, c compared to x, y, z). Error bars show standard errors of the mean

aggregate sizes in different columns. Random root distributions were simulated to address this. For these, the differences in root length densities due to aggregate size vanished, and only significant difference between the genotypes occurred that are proportional to the differences in total root length density (Fig. 2c). Surprisingly, also for the randomized root distributions of WT higher root length density could be found in the sand matrix compared to the loamy aggregates. These differences, however, were small compared to the differences that occurred with the original root system architecture.

The reason for the higher root length density within the sand matrix than within aggregates of the randomized root distributions is the heterogeneous distribution of roots and aggregates within such a column experiment. The pattern revealed by the analysis of root length density and aggregate volume fraction with distance to the column wall (Fig. S3) shows 1) increasing aggregate volumes with increasing wall distance to a plateau after roughly 1.5 mm as these convexly shaped objects cannot fit perfectly to the column wall, whereas 2) roots have the highest root length densities, root volumes and lowest root diameter at a distance of approx. 0.2 mm to the wall as there are on average much smaller than aggregates.

The highest root length densities in the sandy matrix were found in close proximity to aggregates (Fig. 4). Combining all root information from the aggregate distance analysis two root morphological changes became apparent: 1) at a distance of approx.

**Fig. 4** Root distribution around aggregates. Compared are the genotypes of maize (WT = wildtype, *rth3* = root hairless variety) and randomized root distributions of these. Dashed lines point to distances at which morphological changes became apparent. These points of morphological changes are mainly declared based on the peaks in root branch density, which come along with changes in the other measures






0.6 mm to the aggregate boundaries there was a local increase in branching point density. The laterals that emerged from it and grew towards the aggregates caused a reduction in average root diameters at distances  $<0.6$  mm. 2) at a distance of approx. 0.2 mm to aggregates boundaries another peak in branch densities occurred. This led to the aforementioned peak in root length densities but was not associated with a high root volume density, as mean root diameters decreased further towards aggregates. The random root distribution showed almost no trend as a function of aggregate distance. When pooling the continuous

distance into distinctive distance classes (Table 1), the aggregates and their vicinity ( $<0.6$  mm) make up 30% of the total volume, which also roughly corresponds to 30% of all roots for both genotypes.

In addition to penetration resistance, nutrient availability could also have had an impact on root growth. Despite being removed prior to matrix fertilization, P concentrations in aggregates were significantly higher than in the sandy matrix at harvest (Fig. S4). The difference in the P concentration of matrix and aggregates was significantly higher for WT ( $56.3 \text{ mg kg}^{-3}$ ) than for *rth3* ( $45.47 \text{ mg kg}^{-3}$ ,  $p = 0.016$ ).



**Table 1** Pooled continuous distance in distinctive distance classes for both genotypes (WT = wildtype, *rth3* = root hair defective genotype)

	within Aggregates		Aggregate vicinity (<0.6mm distance)		Aggregate + vicinity		Bulk soil (>0.6mm distance)	
	WT	<i>rth3</i>	WT	<i>rth3</i>	WT	<i>rth3</i>	WT	<i>rth3</i>
Relative root  length [%]	1.51 (±0.26)	1.63 (±0.21)	25.50 (±2.47)	26.44 (±0.30)	27.0 (±2.69)	28.07 (±0.2)	73.00 (±2.69)	71.93 (±0.2)
Relative Volume  [%]	10.5 (±0.96)	11.12 (±0.49)	20.78 (±1.59)	21.26 (±1.03)	31.28 (±2.54)	32.43 (±1.25)	68.72 (±2.54)	67.57 (±1.25)
Root  length density [cm cm <sup>-3</sup> ]	0.46 (±0.06)	0.24 (±0.04)	3.97 (±0.35)	2.11 (±0.35)	2.79 (±0.23)	1.47 (±0.24)	3.44 (±0.25)	1.79 (±0.25)

Numbers in brackets depict the standard error

## Discussion

### Local adaption of root growth to overcome soil heterogeneity

This study was set up with the aim to assess the change of root system architecture of maize due to presence of aggregates - which induce heterogeneity in both, penetration resistance and nutrient availability - in comparison to a sieved control in which the same amount of loam is homogeneously mixed into the sand. Penetration resistance information was only available for the sieved substrate (0.08 MPa). However, it can be inferred from complementary information that the penetration resistance of macroaggregates was much higher. In addition, the penetration resistance that the root tip experiences is particularly important for root plasticity, but different from what a rigid penetrometer tip is detecting. The presence of aggregates did not induce significant root or shoot growth differences between the two substrates (Fig. 2). Based on that finding we conclude that maize

plants were able to adapt to the heterogeneity in nutrient availability and penetration resistance caused by the aggregates. However, root length densities were much lower within aggregates compared to the sand substrate (Fig. 3), even after taking into account the lower root recovery rate of 86% inside aggregates they were still less abundant indicating that root ingression into these dense aggregates was impaired. This is in agreement with the exponential decrease of root growth with increasing penetration resistance found in the literature (Bengough et al. 2011; Dexter 1986) and findings of Montagu et al. (2001) who showed that shoot growth in partially compacted soil is maintained, if reduced growth in compacted soil layers is compensated by enhanced root elongation in more loose areas. Previous studies suggested root thickening as a plasticity trait to achieve greater penetration depth in compacted soil (Bengough et al. 2011; Materechera et al. 1992). However, this study did find decreased root diameters at the transition towards the zones of higher penetration resistance (Fig. 4b), i.e. only the smallest roots grew into them (Fig. 4b). The

increase in lateral root growth towards aggregates lead to a peak of root length densities in the direct vicinity of aggregates and simultaneously explains the smaller mean root diameters (Fig. 4a, d). Freitas et al. (1999) showed that once maize roots encounter a pathway between aggregates, they continue growing along the outside of the aggregate unless they find an intra-aggregate pore they can enter. Thus, during the growth around aggregates, roots may also preliminary have followed the existing macropore space, present in the sandy substrate. This would lead to localised radial compression and thus additionally to smaller mean root diameters, compared to roots responding to axial pressure by radial expansion (Bengough 2012).

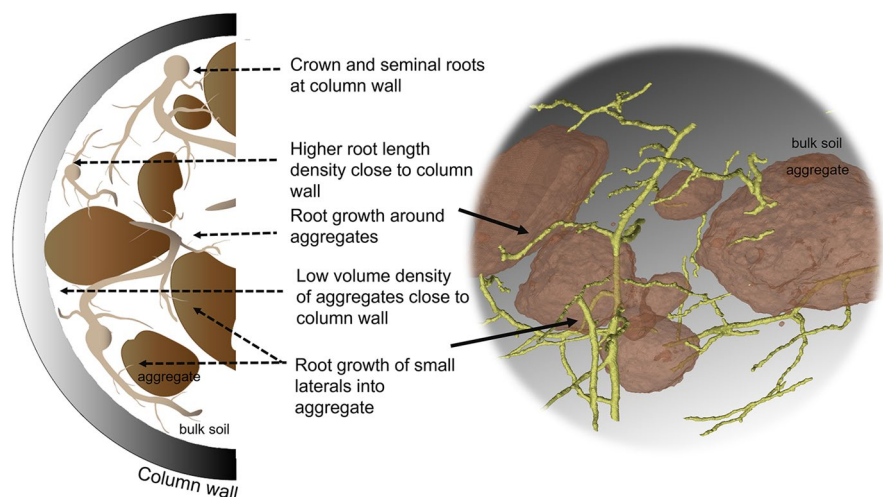
However, the increased root length density was probably only a result of branching and the corresponding accumulation of roots around aggregates, as the pooled length densities of aggregates and the surrounding area was even slightly lower than in the rest of the soil. There are two main reasons for these different root length densities: 1) a pot experiment bias as most roots can be found at the column wall, where no aggregates are found (Fig. S3). Thus, even the random root distributions showed lower root length densities in aggregates compared to the matrix for WT. 2) An imaging bias as WT had a lower root recovery rate compared to *rth3*, because of thinner roots, and thus may also have had a lower recovery within aggregates. However, the general trend of the root diameters, which already started to decrease at a distance of 0.5 cm from the aggregate surface to the lowest values within the aggregates, revealed a general

morphological change, i.e. increased root growth of laterals towards aggregates (Fig. 5). This is in good agreement with the findings of Burr-Hersey et al. (2017), which showed that radish responded to compacted soil by morphological changes, with the single thick taproot branching out into several finer roots that penetrated the denser soil. The increase of root length density around aggregates as a consequence of increased branching (Fig. 4d) could also be an important factor to maintain sufficient nutrient uptake from the P rich aggregates. Nutrient analysis confirmed that there was an incentive for roots to grow towards the aggregates to acquire P. In addition, 3 days before harvest, the aggregated treatments seem to maintain an even higher growth of leaf area for both genotypes compared to their sieved equivalents, i.e., at a time point at which aggregates are already covered by roots. The accumulation of roots on the aggregate surface thus seems to be triggered mainly by the increased penetration resistance, while the increased branching simultaneously ensures sufficient P uptake.

#### The importance of root hairs

For both substrates, the growth of the *rth3* mutant was significantly lower as compared to the wild-type. It developed less than half of the total root length density. These results are in line with results obtained in experiments under similar conditions with the sieved substrate (Ganter et al. 2021; Lipold et al. 2021b). Root growth into the aggregates is clearly hindered, i.e. the relative root length within

**Fig. 5** Scheme of root and aggregate distribution within columns (left) and CT image of small roots enclosing aggregates



aggregates is smaller than the relative volume. This applies equally to both genotypes, which show equal distribution of relative root length (Table 1). The differences in the absolute root length (density) are therefore not due to the fact that *rth3* can penetrate less easily, but rather to a general poorer root and shoot growth of *rth3*. Despite poorer growth of *rth3*, the mutant developed significantly higher root diameters than the wild-type. One reason for root thickening could be the compensation for the lack of root anchorage as root thickening decreases penetration stress and stabilizes roots (Materechera et al. 1992). Another reason for developing thicker roots could be the lower root surface for *rth3*, as the uptake of nutrients strongly depends on a good root to soil contact (Carminati et al. 2013) which suffers from the absence of hairs. This may lead to thicker roots in a substrate with bigger pores and gaps i.e. in the sandy matrix, to increase the root surface for a given unit of root length (Haling et al. 2013). In contrast to our findings, Hill et al. (2006) found a decreased root diameter and increased specific root length in response to P deficiency. Strock et al. (2018) concluded reduced root secondary growth is a response to low P availability. Although the shoot P concentration in this experiment does not differ between the two genotypes, the Ca:P ratio revealed less efficient P uptake for the hairless mutant. This is in line with results obtained in a similar experiment (Lippold et al. 2021b) with both genotypes and the fine sieved substrate in combination with a loamy substrate. Since root length as well as branching density and root diameter of both genotypes behave the same in and around aggregates, it can be concluded that root hairs did not provide a major advantage for the WT compared to *rth3* for the growth into the dense aggregates. However, *rth3* was less well supplied with P, and thus root hairs or the smaller root diameters were beneficial for the P uptake of the WT. Another explanation for increased average diameters could be that in the absence of root hairs, the average diameter of fine roots increased to facilitate arbuscular mycorrhizal fungi colonization (Kumar et al. 2019). In a similar experiment with the fine sieved sandy substrate (Lippold et al. 2021b) first signs of mycorrhizal colonization were found, despite the early growth stage.

## Conclusions

The analyses of root traits in a holistic way, i.e. by describing them with respect to their appearance (abundance and morphology) around aggregates and the column wall, enabled us to assess the change of root system architecture of maize induced by heterogeneity in penetration resistance and nutrient uptake into the shoot (Fig. 5). A substrate containing larger sized loam aggregates mixed into the sand did not induce significant root or shoot growth differences in comparison to a sieved control in which the same amount of loam was homogeneously mixed. Thus, we conclude macroaggregation of loam in sandy soil shows little influence on maize growth, due to local adaptations of root architecture to the heterogeneity in nutrient availability and penetration resistance caused by the aggregates.

The conditions of this experiment may be only expected in anthropogenic soils to the same degree, within mixed substrates. However, macroaggregates formed by e.g. tillage or by earthworms can induce similar heterogeneity under field conditions. Due to the shown mechanisms of root adaptations, roots are able to compensate fully for these local heterogeneities.

**Acknowledgements** Maxime Phalempin helped segmenting the CT images, Sebastian Blaser helped creating 3D images in VG-Studio, Ines Volkmann measured nutrient concentrations in tissue material, EUROFINs Agraranalytik Deutschland GmbH analysed the soil substrate, Franziska Busch helped during harvest of the Experiment as well as with WinRhizo measurements.

**Authors' contribution** DV and EL conceptualized and designed the study. DV and SS acquired the funding. EL and TF conducted the Experiment. ML, EL, TF and SS discussed and evaluated the data. ML and EL wrote the manuscript with the input from SS and DV. All authors provided feedback and approved the final version of the manuscript.

**Funding** Open Access funding enabled and organized by Projekt DEAL. This project was funded by DFG, German Research Foundation (project number 403801423) as part of priority programme 2089 "Rhizosphere spatiotemporal organisation - a key to rhizosphere functions".

**Data availability** The datasets generated during and/or analysed during the current study are available from the corresponding author on reasonable request.

## Declarations

**Conflict of interest/competing interests** The authors have no relevant financial or non-financial interests to disclose.

**Open Access** This article is licensed under a Creative Commons Attribution 4.0 International License, which permits use, sharing, adaptation, distribution and reproduction in any medium or format, as long as you give appropriate credit to the original author(s) and the source, provide a link to the Creative Commons licence, and indicate if changes were made. The images or other third party material in this article are included in the article's Creative Commons licence, unless indicated otherwise in a credit line to the material. If material is not included in the article's Creative Commons licence and your intended use is not permitted by statutory regulation or exceeds the permitted use, you will need to obtain permission directly from the copyright holder. To view a copy of this licence, visit <http://creativecommons.org/licenses/by/4.0/>.

## References

- Becher HH (1992) Die Bedeutung der Festigkeitsverteilung in Einzelaggregaten für den Wasser- und Stofftransport im Boden. *Z Pflanzenernähr Bodenkd* 155:361–366. <https://doi.org/10.1002/jpln.19921550503>
- Bengough AG (2012) Root elongation is restricted by axial but not by radial pressures: so what happens in field soil? *Plant Soil* 360:15–18. <https://doi.org/10.1007/s11104-012-1428-8>
- Bengough AG, McKenzie BM, Hallett PD, Valentine TA (2011) Root elongation, water stress, and mechanical impedance: a review of limiting stresses and beneficial root tip traits. *J Exp Bot* 62:59–68. <https://doi.org/10.1093/jxb/erq350>
- Bengough AG, Loades K, McKenzie BM (2016) Root hairs aid soil penetration by anchoring the root surface to pore walls. *J Exp Bot* 67:1071–1078. <https://doi.org/10.1093/jxb/erv560>
- Blaser SRGA, Koebnick N, Spott O, Thiel E, Vetterlein D (2020) Dynamics of localised nitrogen supply and relevance for root growth of *Vicia faba* ('Fuego') and *Hordeum vulgare* ('Marthe') in soil. *Sci Rep* 10:15776. <https://doi.org/10.1038/s41598-020-72140-1>
- Burr-Hersey JE, Mooney SJ, Bengough AG, Mairhofer S, Ritz K (2017) Developmental morphology of cover crop species exhibit contrasting behaviour to changes in soil bulk density, revealed by X-ray computed tomography. *PLoS One* 12:e0181872. <https://doi.org/10.1371/journal.pone.0181872>
- Carminati A, Vetterlein D, Koebnick N, Blaser S, Weller U, Vogel H-J (2013) Do roots mind the gap? *Plant Soil* 367:651–661. <https://doi.org/10.1007/s11104-012-1496-9>
- Colombi T, Braun S, Keller T, Walter A (2017) Artificial macropores attract crop roots and enhance plant productivity on compacted soils. *Sci Total Environ* 574:1283–1293. <https://doi.org/10.1016/j.scitotenv.2016.07.194>
- Colombi T, Torres LC, Walter A, Keller T (2018) Feedbacks between soil penetration resistance, root architecture and water uptake limit water accessibility and crop growth - a vicious circle. *Sci Total Environ* 626:1026–1035. <https://doi.org/10.1016/j.scitotenv.2018.01.129>
- Correa J, Postma JA, Watt M, Wojciechowski T (2019) Soil compaction and the architectural plasticity of root systems. *J Exp Bot* 70:6019–6034. <https://doi.org/10.1093/jxb/erz383>
- Dexter AR (1986) Model experiments on the behaviour of roots at the interface between a tilled seed-bed and a compacted subsoil. *Plant Soil* 95:123–133. <https://doi.org/10.1007/BF02378858>
- Downie HF, Adu MO, Schmidt S, Otten W, Dupuy LX, White PJ, Valentine TA (2015) Challenges and opportunities for quantifying roots and rhizosphere interactions through imaging and image analysis. *Plant Cell Environ* 38:1213–1232. <https://doi.org/10.1111/pce.12448>
- Flavel RJ, Guppy CN, Tighe MK, Watt M, Young IM (2014) Quantifying the response of wheat (*Triticum aestivum* L.) root system architecture to phosphorus in an Oxisol. *Plant Soil* 385:303–310. <https://doi.org/10.1007/s11104-014-2191-9>
- Freitas PL, Zobel RW, Synder VA (1999) Corn root growth in soil columns with artificially constructed aggregates. *Crop Sci* 39:725–730. <https://doi.org/10.2135/cropsci1999.0011183X003900030020x>
- Ganther M, Vetterlein D, Heintz-Buschart A, Tarkka MT (2021) Transcriptome sequencing analysis of maize roots reveals the effects of substrate and root hair formation in a spatial context. *Plant Soil*. <https://doi.org/10.1007/s11104-021-04921-0>
- Gao W, Blaser SRGA, Schlüter S, Shen J, Vetterlein D (2019a) Effect of localised phosphorus application on root growth and soil nutrient dynamics in situ – comparison of maize (*Zea mays*) and faba bean (*Vicia faba*) at the seedling stage. *Plant Soil* 441:469–483. <https://doi.org/10.1007/s11104-019-04138-2>
- Gao W, Schlüter S, Blaser SRGA, Shen J, Vetterlein D (2019b) A shape-based method for automatic and rapid segmentation of roots in soil from X-ray computed tomography images: Rootline. *Plant Soil* 441:643–655. <https://doi.org/10.1007/s11104-019-04053-6>
- Haling RE, Brown LK, Bengough AG, Young IM, Hallett PD, White PJ, George TS (2013) Root hairs improve root penetration, root-soil contact, and phosphorus acquisition in soils of different strength. *J Exp Bot* 64:3711–3721. <https://doi.org/10.1093/jxb/ert200>
- Hill JO, Simpson RJ, Moore AD, Chapman DF (2006) Morphology and response of roots of pasture species to phosphorus and nitrogen nutrition. *Plant Soil* 286:7–19
- Hochholdinger F, Wen T-J, Zimmermann R, Chimot-Marolle P, Da Costa o Silva O, Bruce W, Lamkey KR, Wienand U, Schnable PS (2008) The maize (*Zea mays* L.) roothairless3 gene encodes a putative GPI-anchored, monocot-specific, COBRA-like protein that significantly affects grain yield. *Plant J Cell Mol Biol* 54:888–898. <https://doi.org/10.1111/j.1365-313X.2008.03459.x>
- Hodge A (2004) The plastic plant: root responses to heterogeneous supplies of nutrients. *New Phytol* 162:9–24. <https://doi.org/10.1111/j.1469-8137.2004.01015.x>



- Kravchenko A, Guber A (2021) Imaging soil structure to measure soil functions and soil health with X-ray computed microtomography. In: Otten W (ed) *Advances in measuring soil health*. Burleigh Dodds Science Publishing, pp 111–138
- Kumar A, Shahbaz M, Koirala M, Blagodatskaya E, Seidel SJ, Kuzyakov Y, Pausch J (2019) Root trait plasticity and plant nutrient acquisition in phosphorus limited soil. *Z Pflanzenernähr Bodenkd* 182:945–952. <https://doi.org/10.1002/jpln.201900322>
- Legland D, Arganda-Carreras I, Andrey P (2016) MorphoLibJ: integrated library and plugins for mathematical morphology with ImageJ. *Bioinformatics* (Oxford, England) 32:3532–3534. <https://doi.org/10.1093/bioinformatics/btw413>
- Lippold E, Kleinau P, Blaser SRGA, Schlüter S, Phalempin M, Vetterlein D (2021a) In soil measurement of radiation dose caused by X-ray computed tomography. *Z Pflanzenernähr Bodenkd* 184:343–345. <https://doi.org/10.1002/jpln.202000276>
- Lippold E, Phalempin M, Schlüter S, Vetterlein D (2021b) Does the lack of root hairs alter root system architecture of Zea mays? *Plant Soil*. <https://doi.org/10.1007/s11104-021-05084-8>
- Logsdon SD (2013) Root effects on soil properties and processes: synthesis and future research needs. In: Timlin D, Ahuja LR (eds) *Enhancing understanding and quantification of soil-root growth interactions*. American Society of Agronomy and Soil Science Society of America, Madison, WI, USA, pp 173–196
- Lucas M, Schlüter S, Vogel H-J, Vetterlein D (2019) Roots compact the surrounding soil depending on the structures they encounter. *Sci Rep* 9:16236. <https://doi.org/10.1038/s41598-019-52665-w>
- Materrechera SA, Alston AM, Kirby JM, Dexter AR (1992) Influence of root diameter on the penetration of seminal roots into a compacted subsoil. *Plant Soil* 144:297–303. <https://doi.org/10.1007/BF00012888>
- de Mendiburu F (2017) *Agricolae*: statistical procedures for agricultural research. In: R package version 1.3-5 [code]. Available at: <https://cran.r-project.org/web/packages/agricolae/>. Accessed 7 June 2021
- Montagu KD, Conroy JP, Atwell BJ (2001) The position of localized soil compaction determines root and subsequent shoot growth responses. *J Exp Bot* 52:2127–2133. <https://doi.org/10.1093/jexbot/52.364.2127>
- Morris EC, Griffiths M, Golebiowska A, Mairhofer S, Burr-Hersey J, Goh T, von Wangenheim D, Atkinson B, Sturrock CJ, Lynch JP, Vissenberg K, Ritz K, Wells DM, Mooney SJ, Bennett MJ (2017) Shaping 3D root system architecture. *Current Biology* : CB 27:R919–R930. <https://doi.org/10.1016/j.cub.2017.06.043>
- Ollion J, Cochenne J, Loll F, Escudé C, Boudier T (2013) TANGO: a generic tool for high-throughput 3D image analysis for studying nuclear organization. *Bioinformatics* (Oxford, England) 29:1840–1841. <https://doi.org/10.1093/bioinformatics/btt276>
- Otsu N (1979) A threshold selection method from gray-level histograms. *IEEE Trans Syst Man Cybern* 9:62–66
- Phalempin M, Landl M, Wu G-M, Schnepf A, Vetterlein D, Schlüter S (2022) Maize root-induced biopores do not influence root growth of subsequently grown maize plants in well aerated, fertilized and repacked soil columns, *Soil and Tillage Research* (in revision)
- Portell X, Pot V, Garnier P, Otten W, Baveye PC (2018) Micro-scale heterogeneity of the spatial distribution of organic matter can promote bacterial biodiversity in soils: insights from computer simulations. *Front Microbiol* 9:1583. <https://doi.org/10.3389/fmicb.2018.01583>
- Rabot E, Wiesmeier M, Schlüter S, Vogel H-J (2018) Soil structure as an indicator of soil functions: a review. *Geoderma* 314:122–137. <https://doi.org/10.1016/j.geoderma.2017.11.009>
- Ritz K, McNicol JW, Nunan N, Grayston S, Millard P, Atkinson D, Gollotte A, Habeshaw D, Boag B, Clegg CD, Griffiths BS, Wheatley RE, Glover LA, McCaig AE, Prosser JI (2004) Spatial structure in soil chemical and microbiological properties in an upland grassland. *FEMS Microbiol Ecol* 49:191–205. <https://doi.org/10.1016/j.femsec.2004.03.005>
- Robinson D (1994a) Tansley review no. 73. The responses of plants to non-uniform supplies of nutrients. *New Phytol* 127:635–674
- Robinson D (1994b) The responses of plants to non-uniform supplies of nutrients. *New Phytol* 127:635–674. <https://doi.org/10.1111/j.1469-8137.1994.tb02969.x>
- Roskopf U, Uteau D, Peth S (2021) Effects of mucilage concentration at different water contents on mechanical stability and elasticity in a loamy and a sandy soil. *Eur J Soil Sci* 73:1–14. <https://doi.org/10.1111/ejss.13189>
- Rueden CT, Schindelin J, Hiner MC, DeZonia BE, Walter AE, Arena ET, Eliceiri KW (2017) ImageJ2: ImageJ for the next generation of scientific image data. *BMC Bioinformatics* 18:529. <https://doi.org/10.1186/s12859-017-1934-z>
- Schindelin J, Arganda-Carreras I, Frise E, Kaynig V, Longair M, Pietzsch T, Preibisch S, Rueden C, Saalfeld S, Schmid B, Tinevez J-Y, White DJ, Hartenstein V, Eliceiri K, Tomancak P, Cardona A (2012) Fiji: an open-source platform for biological-image analysis. *Nat Methods* 9:676–682. <https://doi.org/10.1038/nmeth.2019>
- Strock CF, La Morrow de Riva L, Lynch JP (2018) Reduction in root secondary growth as a strategy for phosphorus acquisition. *Plant Physiol* 176:691–703. <https://doi.org/10.1104/pp.17.01583>
- Tristán-Vega A, García-Pérez V, Aja-Fernández S, Westin C-F (2012) Efficient and robust nonlocal means denoising of MR data based on salient features matching. *Comput Methods Prog Biomed* 105:131–144. <https://doi.org/10.1016/j.cmpb.2011.07.014>
- Veen BW, Boone FR (1990) The influence of mechanical resistance and soil water on the growth of seminal roots of maize. *Soil Tillage Res* 16:219–226. [https://doi.org/10.1016/0167-1987\(90\)90031-8](https://doi.org/10.1016/0167-1987(90)90031-8)
- Vetterlein D, Lippold E, Schreiter S, Phalempin M, Fahrenkamp T, Hochholdinger F, Marcon C, Tarkka M, Oburger E, Ahmed M, Javaux M, Schlüter S (2021) Experimental platforms for the investigation of spatiotemporal patterns in the rhizosphere-laboratory and field scale. *J Plant Nutr Soil Sci*. <https://doi.org/10.1002/jpln.202000079>
- von Schüller H (1969) Die CAL-methode. Eine neue methode zur bestimmung des pflanzenverfügbaren phosphates in böden. *Plant Nutr Soil Sci* 123:48–63